Fibers **2015**, *3*, 151-172; doi:10.3390/fib3020151

OPEN ACCESS

fibers

ISSN 2079-6439

www.mdpi.com/journal/fibers

Article

Electrospun Scaffolds from Low Molecular Weight Poly(ester amide)s Based on Glycolic Acid, Adipic Acid and Odd or Even Diamines

Sara Keiko Murase, Lu ś Javier del Valle * and Jordi Puiggal í*

Chemical Engineering Department, Polytechnic University of Catalonia, Av. Diagonal 647, Barcelona E-08028, Spain; E-Mail: s_keychan@msn.com

***** Authors to whom correspondence should be addressed; E-Mails: luis.javier.del.valle@upc.edu (L.J.V.); Jordi.Puiggali@upc.edu (J.P.); Tel.: +34-93-401-5649 (J.P.); +34-93-401-6684 (L.J.V.); Fax: +34-93-401-7150 (J.P. & L.J.V.).

Academic Editor: Jingwei Xie

Received: 13 March 2015 / Accepted: 4 May 2015 / Published: 12 May 2015

Abstract: Electrospinning of regular poly(ester amide)s (PEAs) constituted by glycolic acid, adipic acid and diamines with five and six carbon atoms has been carried out. Selected PEAs were constituted by natural origin products and could be easily prepared by a polycondensation method that avoids tedious protection and deprotection steps usually required for obtaining polymers with a regular sequence. Nevertheless, the synthesis had some limitations that mainly concerned the final low/moderate molecular weight that could be attained. Therefore, it was considered interesting to evaluate if electrospun scaffolds could still be prepared taking also advantage of the capability of PEAs to establish intermolecular hydrogen bonds. Results indicated that the crucial factor was the control of polymer concentration in the electrospun solution, being necessary that this concentration was higher than 40% (*w/v*). The PEA with the lowest molecular weight (M_w close to 8000 g/mol) was the most appropriate to obtain electrospun samples with a circular cross-section since higher molecular sized polymers show solvent retention problems derived from the high viscosity of the electrospun solution that rendered ribbon-like morphologies after the impact of fibers into the collector. The studied PEAs were semicrystalline and biodegradable, as demonstrated by calorimetric and degradation studies. Furthermore, the new scaffolds were able to encapsulate drugs with anti-inflammatory and bacteriostatic activities like ketoprofen. The corresponding release and bactericide activity was evaluated in different media and against different bacteria. Finally, biocompatibility was demonstrated using both fibroblast and epithelial cell lines.

Keywords: poly(ester amide)s; biodegradable polymers; electrospinning: scaffolds; biocompatibility

1. Introduction

Poly(ester amide)s (PEAs) are nowadays one of the most promising synthetic materials for biomedical applications. Their excellent suitable properties are provided by the ester and amide linkages present in their structure. Ester units are hydrolytically cleavable and permit a better solubility in organic solvents. In addition, amide units improve the thermal and mechanical properties of the polymer, due to the formation of hydrogen bonds between them. The combination of both groups in the same material increases the wide combination paths to obtain multiple new materials with tuneable properties.

The synthetic mechanisms for the preparation of the different PEAs are diverse but can be grouped into a couple, ring-opening polymerization and polycondensation, which includes melt, interfacial and solution polymerization. The final microstructure can also differ between random, segmented or sequential, which results in a higher variability. So, depending on the final application and desired properties, a synthetic route will be chosen. The applications of the different PEAs are wide, also in the biomedical field. Examples are drug delivery microspheres [1–3], tissue engineering [4,5], hydrogels [6], smart materials [7], adhesives [8] and thermosensitive polymers [9], among others.

An easy synthetic method has been developed to obtain poly(ester amide)s composed by a regular sequence involving glycolic acid and ω-amino acid units or alternatively by a sequence composed by glycolic acid, diamine and dicarboxylic acid units (Figure 1). The procedure is based on a thermal polycondensation of a single monomer or two monomers that occurs in the solid or liquefied state through the formation of metal halide salts as the driving force. This method has advantages related to its high yield, the capability to lead regular repeat units that otherwise requires complex syntheses with multiple protection/deprotection steps [10] and, finally, if it is necessary the possibility to obtain highly porous materials after removal of the formed salt. Despite these clear advantages, the method has limitations derived from the moderate molecular weight that can be attained mostly as a consequence of competitive thermal degradation reactions. Therefore, it seems interesting to explore the potential of these biodegradable materials for tissue engineering applications and specifically for those prepared from two monomers, since the achievement of a perfect stoichiometry is an additional difficulty to render high molecular sizes. In particular, PEAs featuring a regular sequence distribution derived from different diamines, such as 1,3-pentanediamine, 1,5-pentanediamine [11], 1,6-hexanediamine and different dicarboxylic acids [12], have already been prepared and characterized. All of them include a glycolic acid unit, which result in higher biodegradable and biocompatible PEAs. The resulting degraded units are glycolic acid residues, molecules already present in the metabolism, which minimize the immune system's response.

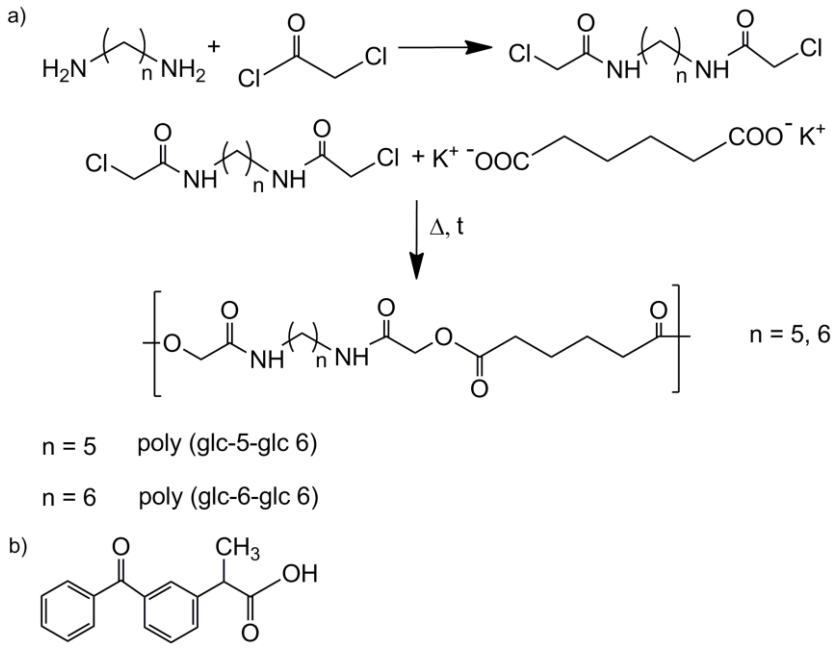

Figure 1. (**a**) Synthesis schemes for poly(ester amide)s derived from glycolic acid, adipic acid and 1,5-pentanediamine (poly(glc-5-glc 6)) or 1,6-hexanediamine (poly(glc-6-glc 6)); (**b**) Molecular structure of ketoprofen (KTP).

The use of natural origin products in the chemical industry is nowadays of great concern. The search for monomers and reagents that can be obtained from natural or microbial resources is a main research topic. In this line of work, 1,5-pentanediamine can be obtained from the amino acid lysine produced by fermentation of plant materials and is used to produce bio-based nylon. For example, nylon 5 6 can be compared in mechanical strength and heat resistance to the one prepared from synthetic hexamethylenediamine [13]. In addition, 1,6-hexanediamine (HDMA) has also been produced from a renewable feedstock using a chemical catalytic process technology. A 100% bio-based nylon 6 6 can be prepared using HDMA and adipic acid (AA) both originated from natural resources under Rennovia RENNLON^{TM} brand [14]. Both bio-based monomers are used to prepare nylon matrices for clothing or membranes. In the present work, both diamines will be used as indicated before to prepare PEAs for tissue engineering applications as electropun scaffolds. The selected diamines differ also on the odd or even number of main chain atoms, which should have an important effect on the intermolecular hydrogen bonding geometry and, therefore, on the final properties.

The electrospinning technique (ES) is currently a conventional method for the preparation of nano or micrometric fibers that can be arranged in a three-dimensional device. The origin of this technique dates from the early 1900s [15–17], but the actual setup was not until 1934, first patented by Anton Formhals [18]. The procedure is based on the application of a high voltage on a prepared polymeric solution between the tip of the solution container and a counter electrode located at a collector, which results in the production of dry continuous fibers. Loading of active substances, such as drugs, proteins or fluorophores, into the prepared scaffolds is achieved by different techniques, *i.e.*, post-spinning modifications, inclusion of the drug or nanoparticles into the electrospinning polymeric mixture, emulsion electrospinning or coaxial electrospinning.

In this work, successful synthesis of PEAs containing the aforementioned diamines is presented using a solid-state polycondensation reaction. Preparation of fibers from the prepared PEAs is accomplished using the electrospinning method with the optimal parameters.

The scaffolds are loaded with an anti-inflammatory drug, ketoprofen (KTP), to demonstrate a possible implementation as drug delivery system (DDS) and the corresponding release experiments are carried out to determine the drug kinetics release in different media. *In vitro* assays for biocompatibility of the prepared scaffolds are performed with two types of cell strains, Vero, an epithelial cell, and COS-7, a fibroblast-cell line. To complement, *in vitro* antimicrobial assays are also conducted. Finally, to determine the potential of the hydrolytically degradable ester bonds present in the material, *in vitro* enzymatic studies are caried out with lipase from *Rhizopus oryzae* and proteinase K from *Tritirachiium album*.

2. Experimental Section

Materials: Reagents 1,5-pentanediamine (95%, cadaverine), 1,6-hexanediamine (98%, HMDA), chloroacetyl chloride (98%), adipic acid (99%), sodium hydroxide (pellet form), potassium hydroxide (≥85% in pellet form) and solvents (formic acid (≥95%) and methanol (≥99.8%)) were purchased from Sigma Aldrich (St. Louis, MO, USA) and used as received. Dry diethyl ether (≥99.8%) and absolute ethanol were purchased from Panreac (Barcelona, Spain) and used as received. Lipase from *Rhizopus oryzae*, proteinase K from *Tritirachiium album*, Dulbecco's phosphate-buffered saline medium and ketoprofen (≥98%, KTP from now on) were also purchased by Sigma Aldrich. The bacterial strains *Escherichia coli* CECT 101 and *Micrococcus luteus* CECT 245 were obtained from the Spanish Type Culture Collection (Valencia, Spain). Vero (epithelial cells derived from African green monkey kidney) and COS-7 (kidney fibroblast cells derived from African green monkey) were purchased from the ATCC (Manassas, VA, USA).

Measurements: ^{1}H-NMR spectra were recorded with a Bruker AMX-300 spectrometer (Wissenbourg, France) operating at 300.1 MHz. Chemical shifts were calibrated using tetramethylsilane as the internal standard and $CDCl_3$ $\delta(^{1}H)$ = 7.26 ppm and deuterated DMSO $\delta(^{1}H)$ = 2.50 ppm as solvents.

Infrared absorption spectra were recorded with a Fourier Transform Infrared Spectrometer (Jasco, model 4100, Tokyo, Japan) in a 4000–600 cm^{-1} range. A Specac-Teknokroma model Golden Gate provided with an attenuated total reflection (Jasco, Tokyo, Japan) with a heated Single Reflection Diamond ATR Top Plate was also employed.

Molecular weights and polydispersity index (PDI) were estimated by size exclusion chromatography (SEC) using a liquid chromatograph (Shimadzu, model LC-8A, Tokyo, Japan) equipped with Waters (Empower). A PL HFIP gel column (Polymer Lab) and a refractive index detector (Shimadzu RID-10A) were employed. The polymer was dissolved and eluted in 1,1,1,3,3,3-hexafluoroisopropanol at a flow rate of 0.5 mL/min. The number and weight average molecular weights were calculated using polymethyl methacrylate standards.

Calorimetric data were obtained by differential scanning calorimetry with a TA Instruments Q100 series equipped with a refrigerated cooling system (RCS). Experiments were conducted under a flow of

dry nitrogen with a sample weight of 2 mg while calibration was performed with indium. Heating runs were carried out at 20 ℃/min rate.

Synthesis of monomers:

(1) ***N,N′*-bis(chloroacetyl)-1,5-pentanediamine (glc-5-glc) and *N,N′*-bis(chloroacetyl)-1,6-hexanediamine (glc-6-glc):** 8.75 mL (0.11 mol) of chloroacetyl chloride were dissolved in 20 mL of dried diethyl ether under nitrogen atmosphere in a previously dried pressure-equalizing dropping funnel. The solution was added dropwise to 50 mL of NaOH 4M solution containing 0.05 mol of 1,5-pentanediamine (for glc-5-glc) or 1,6-hexanediamine (for glc-6-glc) in a round bottom flask magnetically stirred at 0 ℃. pH was maintained around 11 with additional NaOH 4M solution to neutralize the HCl formed during the reaction. After 3 h, the reaction was stopped and the solution filtrated. The recovered precipitate was exhaustively washed with distilled water and diethyl ether. The white powder was vacuum dried at 30 ℃.

(2) **Potassium adipate:** A certain amount of adipic acid was neutralized by an ethanolic solution of KOH 4M. The solution was rotoevaporated and vacuum dried.

(3) **Polymerization of the homopolymers:** An equimolar mixture of potassium adipate and *N,N′*-bis(chloroacetyl)-1,5-pentanediamine or *N,N′*-bis(chloroacetyl)-1,6-hexanediamine was introduced in a reaction tube provided with a magnetic stirrer and pump-filled with nitrogen atmosphere. The reaction tube was heated in an oil bath at 140 ℃ for 5 h or 160 ℃ for 3 h for each mixture, respectively, and stopped introducing the tube in an ice-bath. The polymer was purified by precipitation with methanol of a diluted formic acid solution. The solid was filtrated and repeatedly washed with distilled water, methanol and diethyl ether. Finally, the obtained white powder was dried under vacuum at 30 ℃ for 2 days.

(4) **Poly(glc-5-glc 6):** Yield: 70%. m.p. 118 ℃. M_w: 18,000 g/mol. Polydispersity: 2.4. FTIR (ATR) cm^{-1}: 3270 (Amide A), 3086 (Amide B), 2927 and 2861 (CH_2), 1738 (C=O), 1638 (Amide I), 1540 (Amide II) and 1145 (C-O). ^{1}H-NMR ($CDCl_3$/TFA, TMS as int. ref., ppm): 7.54 (s, 1H, CONH), 4.60 (s, 4H, OC*H*$_2$CO), 3.49 (m, 4H, CONHC*H*$_2$), 2.64 (m, 4H, OOCC*H*$_2$), 1.80 (m, 4H, OOCCH$_2$C*H*$_2$), 1.71 (m, 4H, NHCH$_2$C*H*$_2$) and 1.47 (m, 2H, NHCH$_2$CH$_2$C*H*$_2$).

(5) **Poly(glc-6-glc 6):** Yield: 75%. m.p. 118 ℃. M_w: 7,900 g/mol, Polydispersity: 2.8. FTIR (ATR) cm^{-1}: 3288 (Amide A), 3083 (Amide B), 2937 and 2861 (CH_2), 1744 (C=O), 1654 (Amide I), 1551 (Amide II) and 1142 (C-O). ^{1}H-NMR ($CDCl_3$/TFA, TMS as int. ref., ppm): 7.25 (s, 1H, CONH), 4.82 (s, 4H, OCH$_2$CO), 3.41 (m, 4H, CONHC*H*$_2$), 2.59 (s, 4H, OOCCH$_2$), 1.75 (s, 4H, OOCCH$_2$C*H*$_2$), 1.62 (s, 4H, NHCH$_2$C*H*$_2$) and 1.39 (s, 2H, NHCH$_2$CH$_2$C*H*$_2$).

Electrospinning process: Unloaded and drug loaded PEAs scaffolds were obtained following a protocol for determining solvent, polymer concentration and operational parameters. Basically, solutions were prepared by dissolving the appropriate amount of polymer in 10 mL of 1,1,1,3,3,3-hexafluoroisopropanol. For drug-loaded scaffolds, KTP was also added to the electrospinning solution to achieve KTP/polymer weight ratios of 1% and 5%.

In all cases, the final solution was introduced in a 5 mL syringe (Becton Dickson, Spain) provided with a needle (18G, Terumo, Belgium) connected to an anode, while the collector was connected to the cathode and covered with aluminium film. Needle tip-collector distances were varied from 10 to 25 cm. The voltage was varied between 10 and 30 kV and applied to the target using a high-voltage supply

(Gamma High Voltage Research, ES30-5W, Ormond Beach, FL, USA). Polymer solutions were delivered via a KDS100 infusion syringe pump (KD Scientific, Holliston, MA, USA) to control the mass-flow rate (from 0.5 to 10 mL/h). All electrospinning experiments were conducted in a plastic cabinet located in a fume hood at room temperature.

Morphology of electrospun scaffolds: Carbon coating was accomplished by using a Mitec K950 Sputter Coater (Quorum Technologies Ltd., West Sussex, UK) fitted with a film thickness monitor *k*150x. Samples were visualized at an accelerating voltage of 5 kV. Diameter of electrospun fibers was measured with the SmartTiff software from Carl Zeiss SMT Ltd. (Göttingen, Germany).

Enzymatic degradation: Films of the product were prepared using a hydraulic press with a temperature controller. Samples of 0.5 cm × 0.5 cm were cut, having similar weights. All samples were exposed to 5 mL of saline phosphate buffer (pH 7.4) containing the determined enzyme (lipase or proteinase K) alongside with sodium azide (0.02% (*w/v*)) and calcium chloride (5 mM). Samples were kept at 37 °C in an orbital shaker at 40 rpm. Concentrations of each enzymatic media were 1000 U/mL for lipase and 6 U/mL for proteinase K. These solutions were renewed every 72 h to prevent enzymatic activity loss. At determined times (*i.e.*, 72, 144, 216, 312, 408, 480, 675 and 817 h), samples were taken from the media, washed three times with Milli-Q water and dried in an oven at 30 °C for 24 h to determine the dry weight. All the experiments were conducted in triplicate.

Drug release: Drug release experiments were performed with square pieces of aluminium foil covered with the electrospun PEA (0.5 cm × 0.5 cm). All samples are prepared in triplicate and weighed before the experiment. Samples were introduced in Falkon tubes with 50 mL of Soerensen's buffer (pH 7.4) and a mixture of Soerensen's media with ethanol 70% (*v/v*). The released drug concentration was determined by means of a UV-3600 spectrometer (Shimadzu, Tokyo, Japan) by absorbance measurements at a wavelength of 260 nm that corresponds to the maximum of the absorbance profile. Calibration curves were prepared using different stock solutions of the assayed KTP drug in the two different release media and relating the measured absorbance at 260 nm with the concentration. 1 mL of sample was taken from each tube at predetermined times and replaced with fresh media. The presented results are an average value of the replicates.

Encapsulation efficiency was calculated by measuring the amount of drug incorporated into the scaffold by UV-vis absorbance measurements at a wavelength of 260 nm. To this end, the loaded sample was dissolved in 1,1,1,3,3,3-hexafluoroisopropanol and ketoprofen was extracted with the Soerensen/ethanol mixture.

Antimicrobial test assays: Antimicrobial tests were performed to determine the bacteriostatic effect of the loaded drug. For that, adhesion and growth assays of both *Escherichia coli* (*E. coli*) and *Micrococcus luteus* (*M. luteus*) on the electrospun mats were performed using 24-well culture plates. Electrospun fibers were collected on commercial cover glasses (22 mm × 22 mm), being the resulting mesh perfectly adhered to the glass surface. For subsequent assays each cover glass was cut in four equal portions (11 mm × 11 mm) with a diamont knife. The prepared samples were sterilized by UV radiation during 30 min. The small portions (mesh plus cover slide) were subsequently introduced in 1.5 mL of broth culture Luria-Bertani medium seeded with 10^8 and 10^3 colony-forming units (CFU) to determine bacterial adhesion and bacterial growth, respectively. The cultures were incubated at 37 °C and shaked at 100 rpm. After 24 h (cell growth assays), aliquots of 100 µL were diluted 10 times with distilled water and the absorbance was measured in a micro-plate reader at 595 nm to determine the number of bacteria.

For bacterial adhesion assays, the culture medium was aspirated after incubation of matrices with bacteria for 24 h and the material washed once with distilled water. Then, 0.5 mL of sterile 0.01M sodium thiosulfate was added to each well to detach the adhered bacteria on the surface of the samples (cover slip plus mesh). These were shaken for 2 min and then kept at rest for 30 min. Finally, 500 μL of culture medium were added to the wells and incubated for 24 h more at 37 °C and 100 rpm. The number of adhered bacteria was determined as above indicated. Controls were conducted onto the PS well surface of the tissue culture plate. Each sample was analyzed in triplicate and the results averaged. To determine the variance and significant difference of the samples a one-way ANOVA test and a *t*-test with a 95% ($p < 0.05$) confidence level were performed.

Biocompatibility assays: Cellular adhesion and proliferation on electrospun scaffolds were determined with Vero and COS-7 strain cells. Both strain cells were cultured in Dulbecco's Modified Eagle medium (DMEM) supplemented with 10% fetal bovine serum, 1% penicillin/streptomycin, and 2 mM L-glutamine at 37 °C under a humidified atmosphere with 5% CO_2.

Culture media were changed every 24 h and for sub-culture the cell monolayers were rinsed with phosphate buffer saline (PBS, pH 7.2) and detached by incubation with trypsin-EDTA (0.25%) at 37 °C for 5 min. The cell concentration was determined by counting with a Neubauer camera and using a Trypan Blue 0.4% solution dye. The detached cells with viability ≥95% were used for the assays.

Samples of matrices collected over cover glasses that were subsequently cut as above indicated were placed in a 24-well culture plate and sterilized by UV radiation in a laminar flux cabinet for 30 min. Cover glasses were fixed onto the polystyrene wells by means of a silicone dot (Silbione® MED ADH 4300 RTV, Bluestar Silicones France SAS, Lyon, France). They were then incubated in 1 mL of culture medium under culture conditions for 30 min to stabilize the materials. The media were aspired and the cells were placed on the surface.

In cell adhesion assays aliquots of 50–100 μL containing 5×10^4 cells were seeded on the previously prepared samples. The plates were incubated for 30 min under culture conditions to allow cell attachment. 1 mL of culture medium was added into each well and the plates were incubated for 24 h. Cell viability was then determined by the 3-(4,5-dimethylthiazol-2yl)-2,5-diphenyl-2H-tetrazolium bromide (MTT) assay. Controls were conducted onto the PS well surface as TCPS (tissue culture plate polystyrene). In cell proliferation assays, a similar procedure was used. The seeded aliquots contained 2×10^4 cells and the incubation time was 7 days. Well media was renewed every 48 h. Viability was also determined by the MTT assay. Every sample was prepared with five replicates and results are presented as an average value. A one-way ANOVA test is also performed to determine the variance between the statistical population groups and a *t*-test with a 95% ($p < 0.05$) confidence level to determine the significant difference.

Samples from biocompatibility assays were treated as follows to obtain scanning electron microscope (SEM) images. First, cells were fixed in 2.5% glutaraldehyde-PBS at 4 °C overnight and then dehydrated with different alcoholic stocks (30 °, 50 °, 70 °, 90 ° and 100 °) in sequence and for 30 min each at 4 °C. Finally, all samples were dried under vacuum and covered by a carbon layer for SEM imaging.

3. Results and Discussion

3.1. Preparation of Electrospun Nanofibers of poly(glc-5-glc 6) and poly(glc-6-glc 6)

Morphology of electrospun fibers depends on both solution properties (e.g., viscosity, surface-tension, dielectric constant, volatility, concentration) and operational parameters (e.g., strength of the applied electrical field, tip-collector distance, flow rate) [19,20]. Selection of an appropriate solvent system usually becomes one of the most crucial points of the electrospinning process. However, in the present work, the scope was limited due to the scarce solubility of the studied polymers in most organic solvents and the need to proceed at a high polymer concentration. The first was derived from the capability to establish strong hydrogen bonding interactions, whereas the second was a consequence of the low/moderate molecular weight of samples. It is well-known that electrospinning requires a minimum molecular weight to form suitable fibers (e.g., poly(ethylene glycol) could not be electrospun when M_n was close to 10,000 g/mol) [21] or alternatively a high molecular weight sample must be added as a supporting polymer [22,23]. Specifically, experiments were performed using 1,1,1,3,3,3-hexafluoroisopropanol as unique solvent while the polymer concentration was varied in the 5%–50% (*w*/*v)* range. Flow rate, voltage and needle-collector distance were also varied in a wide range to produce optimum morphologies.

Typical morphologic defects were observed during the optimization process (Figures 2 and 3), being electrospraying, formation of beads, solvent retention and fiber disruptions detected in most of the assayed conditions. Poly(glc-5-glc 6) was the most problematic sample despite having a higher molecular weight than the 1,6-aminohexanoic derivative as a consequence of its high solvent retention. Thus, drops were usually obtained (Figure 2) and even the best preparation corresponded to fibers that had a flat ribbon appearance even after evaporation of the retained solvent. Fiber with a circular cross-section were formed more easily from poly(glc-6-glc 6), although solvent retention was also detected in some cases as shown in Figure 3.

Flat ribbon like morphologies has been observed for different polymers (e.g., cellulose acetate [24], nylon 11 [25], chitosan/polylactide blends [26], polyvinyl alcohol [27]), with different causes being established for such appearance. For example, a rapid vaporization of the solvent within the electrospinning jet may lead to the formation of a skin layer which later collapses [23,24]. It has also been postulated that the fiber morphology may depend on the flow rate and specifically flat ribbons seem to be favoured at rates so high that the thin fiber walls become unable to support the increasing fiber diameter and collapse to form the flat ribbons [25]. Finally, it has also been reported that highy viscous solutions may difficult solvent evaporation in such a way that relatively wet fibers reach the collector and become flattened by the impact [26]. In our case, this seems to be the main reason, taking also into account the self-aggregation trend through hydrogen bonding of PEAs, which can be enhanced upon cooling (*i.e.*, it occurs when the polymer jet accelerates toward the collector) or during solvent evaporation. The different morphologies observed for 1,5-pentanediamine and 1,6-hexanediamine derivatives can then be well justified considering the distinct molecular weights of the samples. The solvent evaporation rate should increase as the molecular weight was reduced allowing that dried fibers reached the collector and could keep their circular cross-section.

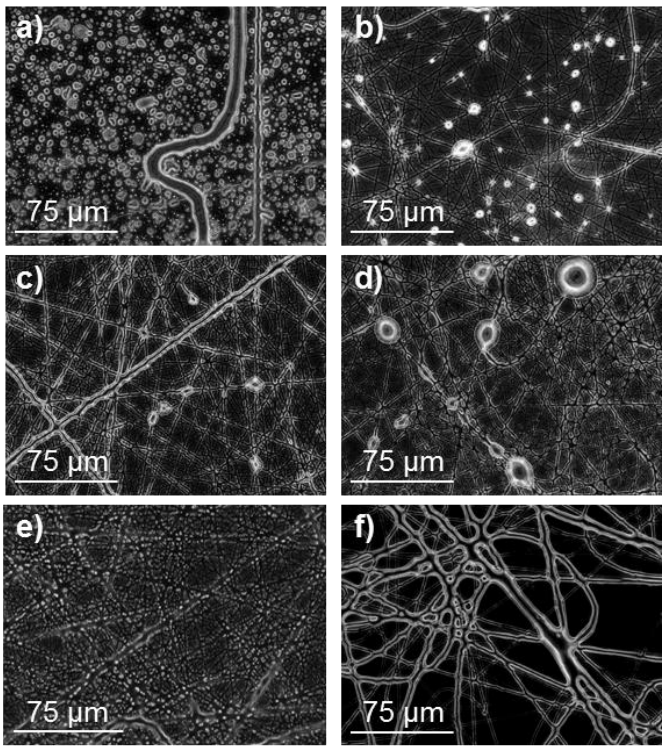

Figure 2. Optical micrographs of (poly(glc-5-glc 6) electrospun samples obtained under the following concentration, flow rate, voltage and needle-collector distance conditions: (**a**) 5% (*w*/*v*), 1 mL/h, 40 kV, 20 cm; (**b**) 10% (*w*/*v*), 1 mL/h, 40 kV, 20 cm; (**c**) 20% (*w*/*v*), 1 mL/h, 10 kV, 12.5 cm; (**d**) 20% (*w*/*v*), 1 mL/h, 20 kV, 20 cm; (**e**) 30% (*w*/*v*), 1 mL/h, 20 kV, 20 cm and (**f**) 50% (*w*/*v*), 4 mL/h, 20 kV, 20 cm.

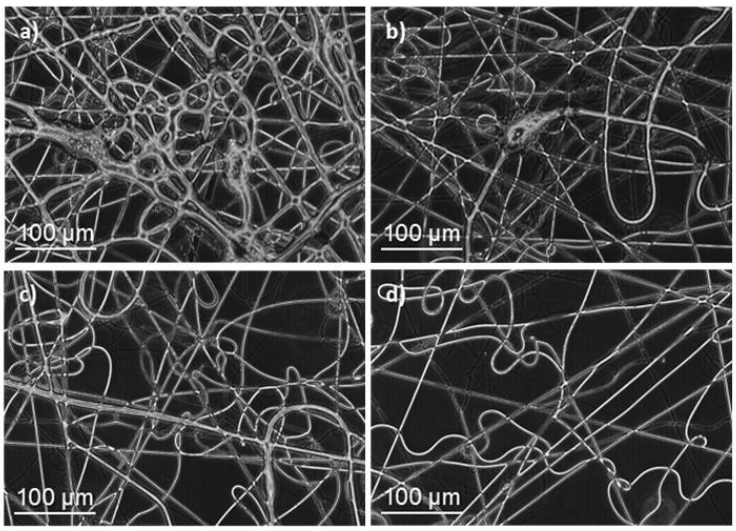

Figure 3. Optical micrographs of poly(glc-6-glc 6) electrospun samples obtained under the following concentration, flow rate, voltage and needle-collector distance conditions: (**a**) 50% (*w*/*v*), 3 mL/h, 15 kV, 20 cm; (**b**) 50% (*w*/*v*), 1.5 mL/h, 10 kV, 20 cm; (**c**) 50% (*w*/*v*), 1 mL/h, 20 kV, 29 cm and (**d**) 50% (*w*/*v*), 1 mL/h, 15 kV, 20 cm.

In general, electrospinning of PEAs led to droplet formation when low polymer concentrations were chosen, as shown in Figure 2 for the 1,5-pentanediamine derivative. Note that a great proportion of drops was observed at the lowest assayed polymer concentration, 5% (*w*/*v*), Figure 2a and that they were still clearly present up to concentration of 20% (*w*/*v*) (Figure 2b–d). In order to enhance solvent evaporation, the needle-collector distance was quickly set to a large value (*i.e.*, 20–30 cm). Nanofibers with a small diameter were generally obtained under most of the assayed conditions. To avoid this feature, voltage was limited to 20 kV but the flow rate could not be highly increased as a consequence of a worse solvent evaporation. Figure 2e,f show the adverse effect (retention of solvent) caused by the use of a high rate. Table 1 reports the experimental conditions that led to the best fiber morphology.

Table 1. Optimal conditions and diameters of unloaded and drug loaded electrospun PEA fibers [a].

Sample	Polymer Concentration (%)	Flow Rate (mL/min)	Voltage (kV)	Diameter [b] (nm)
Poly(glc-5-glc 6)	40	1	20	370, 630
Poly(glc-5-glc 6) + 1% KTP	40	1	20	410, 600
Poly(glc-5-glc 6) + 5% KTP	40	1	20	430, 590
Poly(glc-6-glc 6)	50	0.5	15	500, 2300
Poly(glc-6-glc 6) + 1% KTP	50	0.5	15	510, 1800
Poly(glc-6-glc 6) + 5% KTP	50	0.5	15	520, 1500

Notes: [a] Fibers were obtained using a needle tip-collector distance of 20 cm; [b] Mode (left) and maximum significant value (right).

The lower molecular weight of the 1,6-hexanediamine derivative forced to use a high polymer concentration (50% (*w*/*v*)) to obtain fibers with appropriate morphology. In this case, viscosity of the electrospun solution was not too big to hinder solvent evaporation, if the flow rate was moderate (Figure 3). Note that retention of solvent was again detected when rates were higher than 1 mL/min (Figure 3a,b). Fibers were not significantly improved when needle collector distance and voltage increased from 20 cm and 15 kV, respectively (Figure 3c,d). To sum up, continuous fibers with a circular cross-section could be obtained, as previously indicated, under selected conditions (Table 1). SEM micrographs (Figure 4) revealed that fiber diameters were in a wide range that covered both micrometric (from 0.4 to 2.3 μm) and nanometric (from 60 to 100 nm) scales. Diameter distribution curves for microfibers were highly asymmetric with a great tail for largest values and a mode of 0.5 μm (inset of Figure 4). This feature is in agreement with the reported trend of obtaining bimodal diameter distributions when high polymer concentrations are employed. Micrographs show also that the texture of thicker fibers was characterized by the presence of small pores that could be linked to the indicated problems with the evaporation of the solvent. In addition, it should be pointed out the web-like appearance is caused by the binding during electrospinning of still wet fibers.

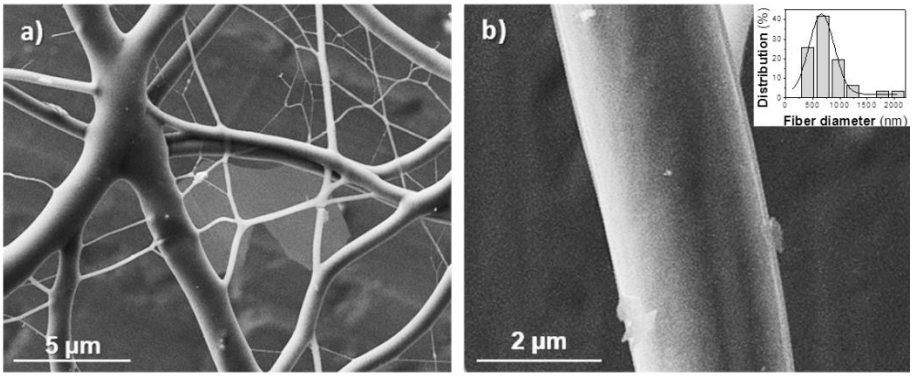

Figure 4. SEM micrographs of (poly(glc-6-glc 6) electrospun samples taken at low (**a**) and high magnification (**b**). Fibers were obtained under the following concentration, flow rate, voltage and needle-collector distance conditions: 50% (*w*/*v*), 0.5 mL/h, 15 kV, 20 cm. The inset shows the diameter distribution of the thicker fiber population.

3.2. Spectroscopic and Calorimetric Data of Poly(glc-5-glc 6) and poly(glc-6-glc 6) Samples

FTIR spectra of the two studied samples show clear differences on the wavenumber associated to the main amide and ester bands whereas the methylene absorption bands appeared at practically the same position (Figure 5). Amide A band (NH stretching) appeared at 3290 and 3280 cm^{-1} for the even and odd diamine derivative, respectively, suggesting that hydrogen bonds were better established in the poly(glc-5-glc 6) sample. In addition, the shape of this Amide A band was clearly different and, specifically, it was narrowest for the even derivatives, a feature that may be related to its lower molecular weight and the existence of a single type of hydrogen bonds. Nevertheless, a shoulder close to 3400 cm^{-1} associated to free amine groups, was detected for both PEAs.

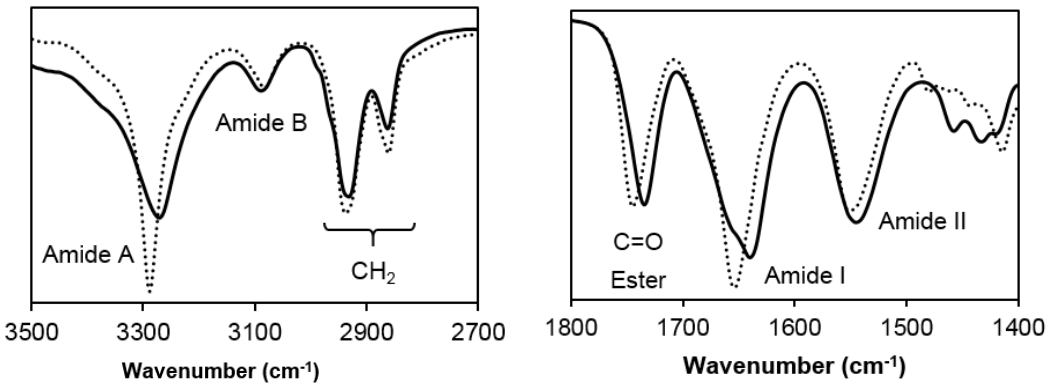

Figure 5. FTIR spectra of the two synthesized homopolymers: Poly(glc-5-glc 6) shown as a continuous line and (poly(glc-6-glc 6)) as a dotted line.

It is well known that polyamides adopt different crystalline structures depending on the number of carbon atoms (*i.e.*, even or odd) of their repeat units. For example, the capability to align the N–H and C=O groups of neighbouring chains with an all-trans molecular conformation should diminish for repeat units involving odd diamines instead of even diamines. This observation contrasts with the FTIR data of the studied PEAs, suggesting that different molecular conformations (e.g., extended or pleated forms)

are involved. The Amide I band was splitted in two (1655 and 1630 cm^{-1}) in the spectra of poly(glc-5-glc 6) as a clear evidence of the coexistence of different structures while a single band (1655 cm^{-1}) was observed in the spectrum of the even derivative. The wavenumber indicated again the establishment of weaker hydrogen bonds for the latter sample. Finally, it is also noticeable that C=O ester groups appeared at slightly different positions (1750 and 1735 cm^{-1} for even and odd derivatives, respectively), pointing out that structural differences concerned also the ester moieties and specifically that stronger intermolecular interactions were established in the odd derivative.

Thermal properties of both PEAs depended on the sample preparation method as shown in the DSC traces depicted in Figures 6 and 7. Some specific issues can be pointed out:

(1) Both samples were semicrystalline and had a relatively high degree of crystallinity. Note the high melting enthalpies (78.4 J/g and 55.6 J/g) determined for samples precipitated from solution. The amorphous character was defined by intermediate glass transition temperature values (*i.e.*, −3 ℃ and 26 ℃ for 1,5-pentenediamine and 1,6-hexanediamine derivatives, respectively) with respect to the ones observed for aliphatic polyamides and polyesters.

(2) Melting behaviour was complex since different peaks were always detected. The predominant one appeared at 100 ℃ and 117–119 ℃, the higher value corresponding to the 1,6-hexanediamine derivative. These differences are in agreement with the well-known odd-even effect that reflects structural differences according to the parity and that is characteristic of nylons and aliphatic polyesters. Note that an increase on the number of methylene groups should give a decrease on the melting temperature if crystalline structure was not changed. Both samples showed also a broad peak at a lower temperature (*i.e.*, 60–70 ℃) that strongly depends on the preparation method (e.g., solution crystallization, solvent casting or electrospinning) and that should be associated with very defective crystals. The predominant melting peak of the 1,6-hexanediamine derivative appears aplitted up (117 ℃ and 119 ℃) in some conditions probably as a consequence of the existence of different lamellar populations that experiment reordering processes during heating. Note, for example, that reordering should be more important for melt-quenched samples and, consequently, the intensity of the corresponding peak at 119 ℃ became the highest.

(3) Enthalpy of the main melting peak clearly diminished when samples were prepared by solvent casting from 1,1,1,3,3,3,-hexafluoroisopropanol solution and chiefly when they were electrospun from the same solvent. The change was dramatic for the 1,5-pentanediamine derivative whose electrospun fibers had the highest solvent retention capability. Specifically, Figures 6 and 7 clearly showed the higher decrease of the area of the melting peak for the electrospun 1,5-pentanediamine derivative, which means a clearly lower capability of this sample to crystallize during electrospinning regarding the even derivative.

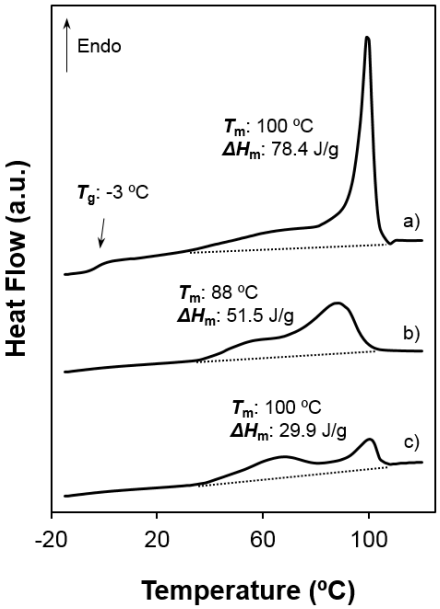

Figure 6. Heating scans of different poly(glc-5-glc 6) samples: (**a**) as-synthesized powder; (**b**) film prepared from solvent casting of a 1,1,1,3,3,3-hexafluoroisopropanol solution and (**c**) electrospun scaffold. Melting enthalpies are given for the overall set of endothermic transitions.

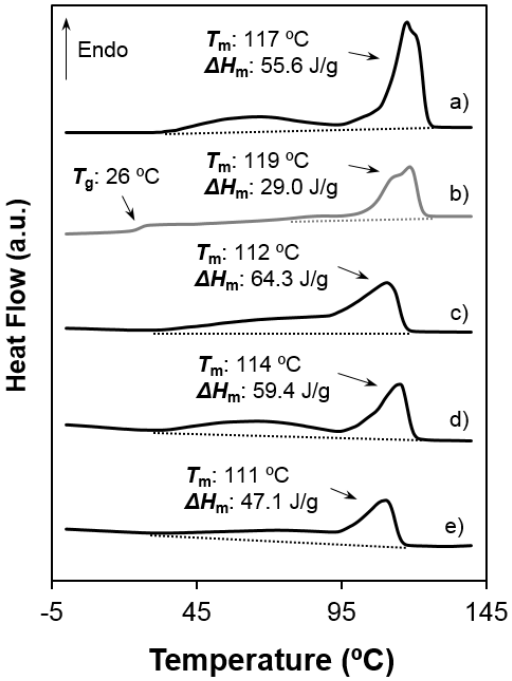

Figure 7. Heating scans of different poly(glc-6-glc 6) samples: (**a**) as-synthesized powder; (**b**) the same melt quenched sample; (**c**) film prepared from solvent casting of a 1,1,1,3,3,3-hexafluoroisopropanol solution; (**d**) electrospun scaffold and (**e**) electrospun scaffold loaded with 5% (*w*/*w*) of ketoprofen. Melting enthalpies are given for the overall set of endothermic transitions.

3.3. Degradation of Poly(glc-6-glc 6) Film Samples

Degradability of PEAs has been evaluated under physiological conditions using a PBS medium as well as enzymatic media. Lipase and proteinase K have been considered in order to have well-differentiated activities. Thus, the former enzyme is only specific to ester bonds, and the second attacks preferentially amide bonds but can also cleave ester bonds.

Figure 8 shows the high influence of the media on the degradation rate of the lower molecular weight sample (*i.e.*, poly(glc-6-glc 6)). Thus, a weight loss of only 15% was observed after 817 h of exposure to the hydrolytic medium. All weight loss was practically produced at the beginning of exposure due to fast solubilization of the smallest molecules. Thus, 11% was measured after only 150 h, while the same exposure period was required to have an additional loss of only 2%. On the contrary, proteinase K was highly effective and rendered a complete degradation after only 600 h. Note that at the beginning, degradation of proteinase K was only slightly higher than that observed for the hydrolytic medium (*i.e.*, 11% respect 8% after 80 h) until it then increased exponentially (e.g., 22%, 37% and 57% determined for 150 h, 217 h and 312 h of exposure). Lipase was clearly less effective since a weight loss of only 20% was determined after 817 h. Nevertheless, a slow but steadily weight loss was detected after the initial period where solubilization of small fragments took place (*i.e.*, an increase from 15% to 20% detected at 216 h and 817 h).

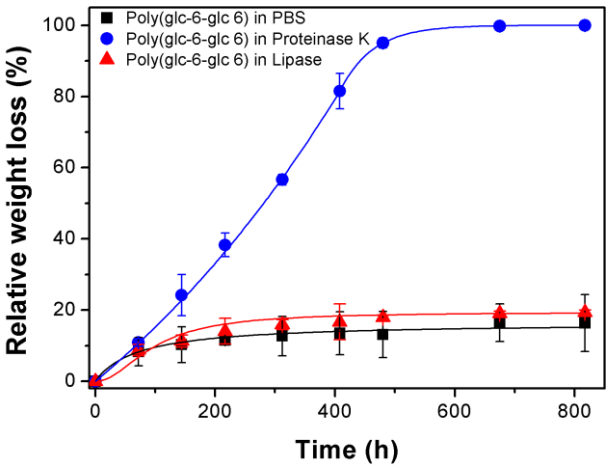

Figure 8. Plot of relative weight loss *versus* exposure time for poly(glc-6-glc 6) films exposed to PBS, proteinase K and lipase media.

Results clearly indicated that the low molecular weight PEA was still sufficiently resistant to hydrolytic degradation for being used in biomedical applications that require a low exposure time and that it could be efficiently degraded by proteolytic enzymes.

Figure 9 compares the film surface attack after 217 h of exposure in the different media. The surface is practically smooth when exposed to the non-enzymatic PBS medium, while a roughness surface produced by erosion is clearly visible in samples exposed to both lipase and proteinase K media. The smooth texture observed for PBS exposed samples points out that weight loss was a consequence in this case of diffusion and solubilization of smaller molecules. Note the different texture of samples exposed to PBS and lipase media for the small period of 217 h (Figure 9a,b), which clearly demonstrated the enzymatic surface attack caused by lipase despite the weight loss was similar (*i.e.*, 12% and 15%).

Texture changes were logically more dramatic for proteinase K exposed samples (Figure 9c,d), being observed the formation of deep cavities after only 312 h of exposure (Figure 9d,e).

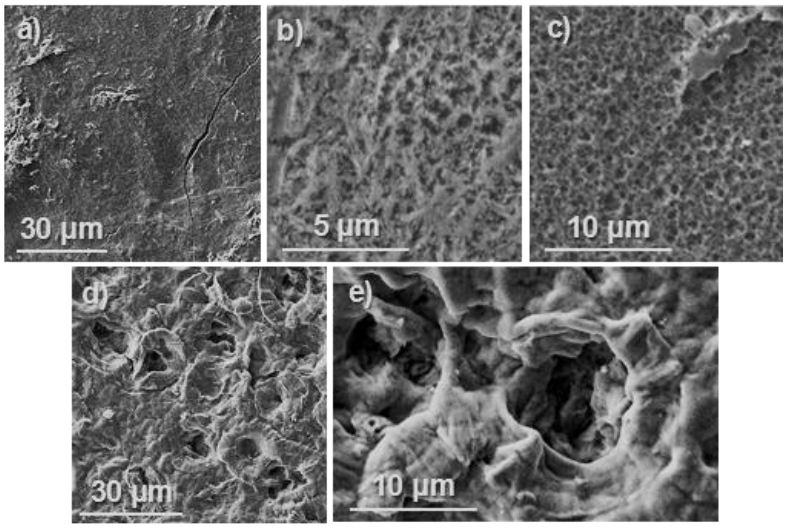

Figure 9. SEM micrographs showing surface texture of poly(glc-6-glc 6) films exposed to PBS for 408 h (**a**); lipase for 217 h (**b**); proteinase K for 217 (**c**) and 312 h (**d**). A high magnification image of the latter is also provided (**e**).

3.4. Load and Release of Ketoprofen in Poly(glc-5-glc 6) and Poly(glc-6-glc 6) Electrospun Samples

Ketoprofen was loaded into the electrospun fibers not only due to their well-known anti-inflammatory effect, but also due to their bacteriostatic activity. In this sense, a fast release from the loaded samples would be convenient. The incorporation of small amounts of ketoprofen to the electrospinning solution did not greatly affect to the final morphologies and consequently the selected processing parameters for unloaded samples could be kept. Diameter distribution data only indicated a slight increase of the mode (*i.e.*, from 370 to 430 nm and from 500 to 520 nm for the 1,5-pentanediamine and the 1,6-hexanediamine derivatives, respectively) and a narrower distribution (*i.e.* the maximum diameter decreased from 630 to 590 nm and from 2300 nm to 1500 nm for the 1,5-pentanediamine and the 1,6-hexanediamine derivatives, respectively) when the amount of loaded KTP increased.

Encapsulation efficiency (*EE*) was close to 32% for samples prepared from solutions containing 5% of KTP (*i.e.*, 34% and 31% for 1,5-pentanediamine and 1,6-hexanediamine derivatives, respectively). Efficiency was dependent on the KTP concentration and logically a higher value was observed for samples obtained from the 1% solution. Specifically, 54% and 63% were determined for poly(glc-5-glc 6) and poly(glc-6-glc 6) scaffolds, respectively.

The incorporation of KTP into the electrospun fibers had also a slight effect on thermal properties since both melting temperature of the main peak and the overall melting enthalpy decreased (see Figure 7d,e for poly(glc-6-glc 6)). These features suggest that a small ratio of KTP could also be incorporated into the crystalline domains and probably could be retained better during release experiments.

Plots of KTP release in the two assayed media from the two electrospun matrices are depicted in Figure 10.

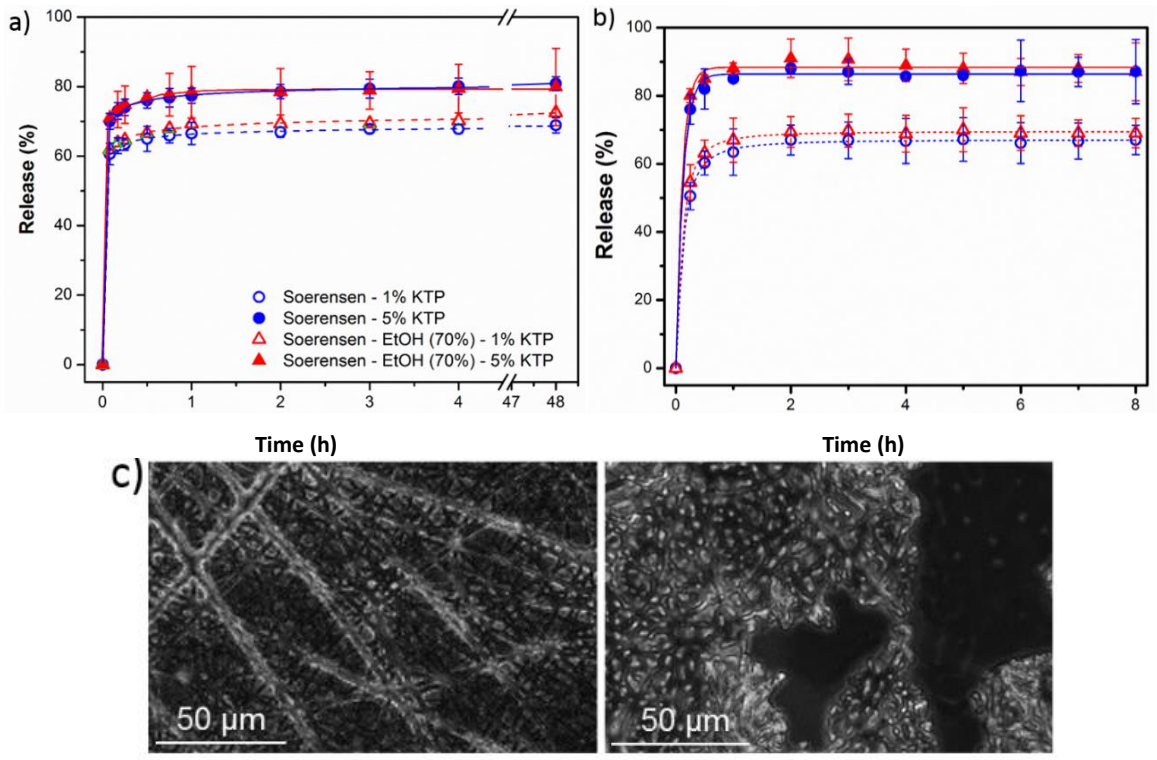

Figure 10. Ketoprofen release curves in Soerensen and Soerensen supplemented with ethanol 70% (*v*/*v*) from poly(glc-5-glc 6) (**a**) and poly(glc-6-glc 6); (**b**) scaffolds loaded with 1% and 5% of the drug. (**c**) optical microscopy images of poly(glc-5-glc 6) scaffolds before (left) and after (right) the release process.

Some points can be discussed:

Most of the loaded drug was quickly released, being required only 1–2 h to achieve the maximum value. This short period allows discarding a degradation effect as also corroborated by the integrity of scaffolds after exposure (Figure 10c) and the above indicated degradation data. In fact, the release profile with a significant burst effect appears typical of a diffusion controlled delivery system.

(1) A small percentage of the loaded drug was effectively trapped into the electrospun fibers, being the value higher when the drug loaded percentage was lower (e.g., 28%–30% and 13%–17% were determined for samples loaded with 1% and 5%, respectively). Probably some molecules were incorporated and effectively trapped in the crystalline domains, being the amount of KTP that could be incorporated in such domains limited. Therefore the release percentage increased with the drug load. Note also that diffusion of KTP from the crystalline arrangement is expected to be hindered. The increase in hydrophobicity of the medium (*i.e.*, addition of ethanol) had a slight influence on the release behaviour, being only detected a small increase of the release percentage when samples were loaded with the lower amount of KTP (*i.e.*, when the percentage of trapped molecules was higher).

(2) Release behaviour was similar for the two matrices despite having different morphologies (e.g., fiber size and cross-sections), molecular weights and chemical structures.

3.5. Bactericide Activity of Ketoprofen Loaded Poly(glc-5-glc 6) and poly(glc-6-glc 6) Electrospun Samples

Antibacterial activity of KTP loaded electrospun scaffolds was tested against *M. luteus* and *E. coli* bacteria (as representative of Gram-positive and Gram-negative bacteria, respectively). Figure 11 shows the quantitative results attained in the bacterial adhesion and growth experiments.

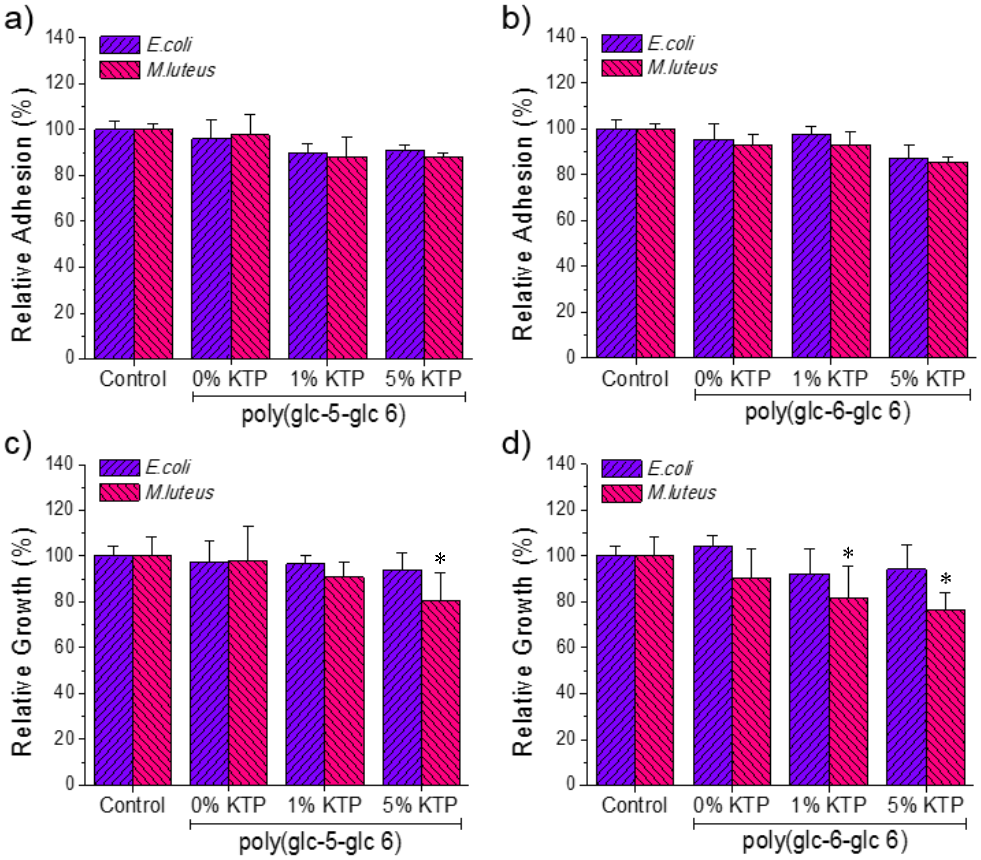

Figure 11. Results of bacterial adhesion (**a**,**b**) and proliferation (**c**,**d**) assays performed on the prepared poly(glc-5-glc 6) (**a**,**c**) and poly(glc-6-glc 6) (**b**,**d**) scaffolds using *E. coli* and *M. luteus.* *$p < 0.05$ *versus* control.

A slight tendency to decrease bacterial adhesion was observed in samples loaded with KTP (Figure 11a,b). Main differences with respect to the positive control and the unloaded samples were observed for bacterial growth assays performed with *M. luteus* and using the poly(glc-6-glc 6) matrix. In this case, a slight bacteriostatic activity could be inferred, being the effect similar for scaffolds loaded with KTP percentages of 1% and 5%. Specifically, the relative growth decreased from 90% (unloaded scaffold) to 80% (1% of KTP) and 75% (5% of KTP) (Figure 11d). Results for the poly(glc-5-glc 6) matrix were less clear since relative growth only decreased for the sample loaded with 5% of KTP, being the percentage even close to that determined for the unloaded sample (*i.e.*, 80% with respect to 98% as shown in Figure 11c). It is widely recognized that the KTP has an inhibitory activity of cyclooxygenase, but like other NSAIDs (non-steroidal anti-inflammatory drugs) also attributed secondarily some antibacterial activity whose mechanism is not clear [28,29].

3.6. Biocompatibility of Poly(glc-5-glc 6) and Poly(glc-6-glc 6) Electrospun Samples

Adhesion and proliferation tests with epithelial (Vero) and fibroblast (COS-7) cell lines were performed on loaded and unloaded scaffolds of both PEAs. These assays are useful in following cell development because adhesion is an early cellular event and proliferation is an evidence of metabolic cell activity. In general, both adhesion and proliferation of COS-7 cell line on all electrospun scaffolds and the control were rather similar (Figure 12).

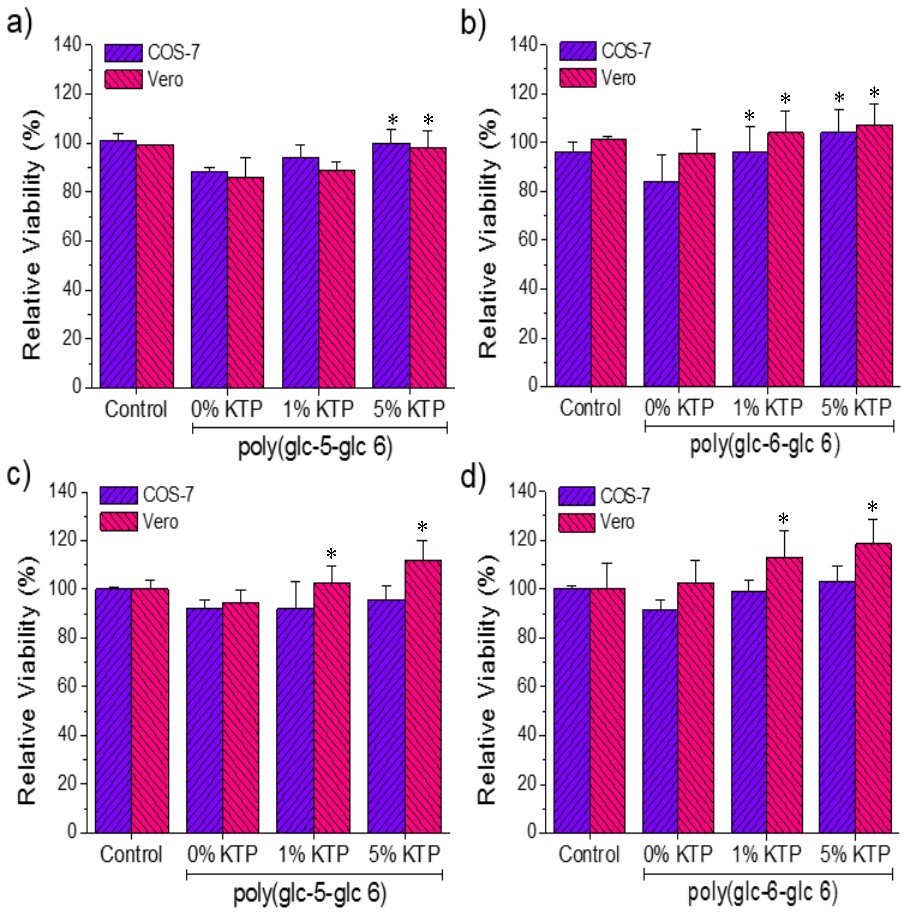

Figure 12. Results of the cellular adhesion (**a**, **b**) and proliferation (**c**, **d**) of COS7 and VERO on the surface of poly(glc-5-glc 6) (**a**,**c**) and poly(glc-6-glc 6) (**b**,**d**) electrospun scaffolds. *$p < 0.05$ *versus* unloaded matrix (0% KTP).

Therefore, the two PEAs seem to be biocompatible, and the loaded KTP did not cause any toxic response even at the highest studied concentration. A slight decrease (close to 20% as can be seen in Figure 12a,b) on the adhesion onto unloaded scaffolds with respect to the control was detected for COS-7 cells, this higher sensitivity probably caused by the requirements imposed by their adherent morphology. Adhesion was increased when samples were loaded with KTP, being the value close to 10% for samples from solutions including 5% of KTP (Figure 12a,b). The positive effect of KTP was more clearly detected in proliferation assays using Vero cells, being the increase with respect to the unloaded matrix around 20%–30% (Figure 12c,d).

Representative micrographs of morphological characteristics of cell growth on electrospun scaffolds are shown in Figures 13 and 14. Fibroblast (COS-7) and epithelial (Vero) cells formed monolayers on

the scaffold surface independently of the KTP loading. Cells were structured with close interactions between them to form a tissue (Figures 13c,d and 14b for COS-7 cells and Figure 14d for Vero cells). Extensions of *lamellipodia* (cell projections), which support cell attachment onto the material surface through *filopodia* (cytoplasmatic projections), were detected on different samples (e.g., see arrows in Figures 13a,b and 14a,b). Fiber tracks can be clearly seen below both COS-7 and Vero cell monolayers grown over poly(glc-6-glc 6) scaffolds (see asterisks in Figure 14a,d).

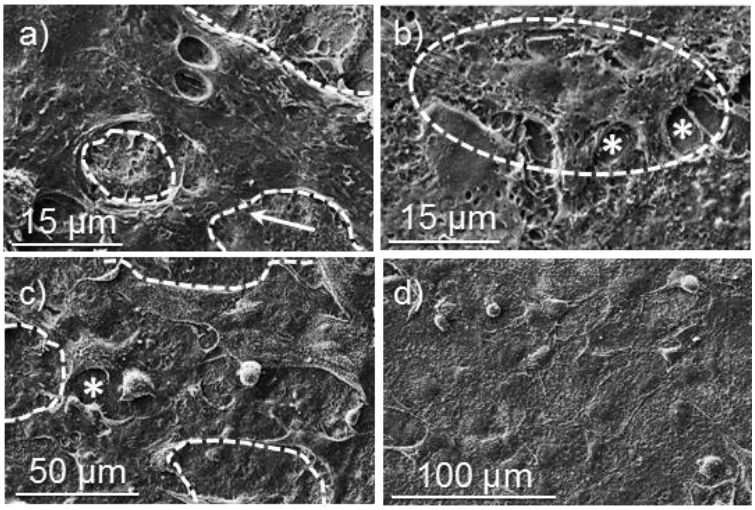

Figure 13. SEM micrographs showing cellular adhesion and proliferation on surfaces of poly(glc-5-glc 6) electrospun scaffolds: (**a**) COS-7 cell adhesion on an unloaded sample; (**b**) VERO cell adhesion on an unloaded sample; (**c**) COS-7 cell proliferation on an unloaded sample; (**d**) COS-7 cell proliferation on loaded samples prepared from 5% KTP electrospinning solution. Dashed lines highlight cell profiles except for (**d**) where a monolayer was formed.

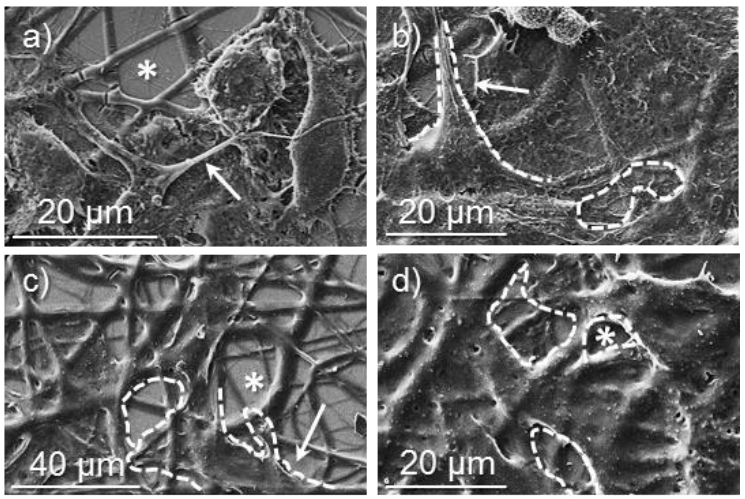

Figure 14. SEM micrographs showing cellular adhesion and proliferation on surfaces of poly(glc-6-glc 6) electrospun scaffolds: (**a**) COS-7 cell adhesion on an unloaded sample; (**b**) COS-7 cell proliferation on a sample loaded from 5% KTP containing electrospun solution; (**c**) VERO cell adhesion on an unloaded sample; (**d**) VERO cell proliferation on an unloaded samples. Dashed lines highlight cell profiles.

4. Conclusions

Low molecular weight samples of poly(glc-5-glc 6) and poly(glc-6-glc 6) could be effectively electrospun from highly concentrated solutions in 1,1,1,3,3,3-hexafluoroisopropanol. Better results were obtained from the sample with the lowest molecular size since the derived solutions had a lower viscosity, and retention of solvent was minimized. The corresponding fibers showed a circular cross-section that contrasted with the ribbon-like fibers obtained when samples with higher molecular samples were produced.

The two studied PEAs had different crystalline arrangements, as could be deduced from the shifts of main amide and ester groups in the FTIR spectra, as well as from the typical odd-even effect observed in thermal analysis. PEAs degraded in enzymatic media, at a higher rate when enzymes could attack both amide and ester groups.

Scaffolds of these new PEAs could be loaded with KTP without changing the operational parameters determined for each polymer. Loaded samples showed a fast release that was slightly dependent on the assayed media (*i.e.*, Soerensen or the Soerensen/ethanol mixture), although a small proportion of the drug was trapped in the more crystalline domains. Loaded samples had a slight bacteriostatic effect against gram-positive *M. luteus* bacteria. Unloaded and KTP loaded scaffolds were biocompatible, with enhanced proliferation of epithelial Vero cells with respect to positive control when scaffolds were loaded with KTP.

Acknowledgments

Authors are in debt to supports from MINECO and FEDER (MAT2012-36205) and the Generalitat de Catalunya (2014SGR188). S.K.M. acknowledges an FPI grant from MICINN.

Author Contributions

The manuscript was finalized through contributions from all authors, and all authors also approved the final manuscript. Conflicts of Interest The authors declare no conflict of interest.

Conflicts of Interest

The authors declare no conflict of interest.

References

1. Qian, Z.; Li, S.; He, Y.; Zhang, H.; Liu, X. Preparation of biodegradable polyesteramide microspheres. *Colloid Polym. Sci.* **2004**, *282*, 1083–1088.
2. Ostacolo, L.; Russo, P.; de Rosa, G.; La Rotonda, M.I.; Maglio, G.; Nese, G.; Spagnuolo, G.; Rengo, S.; Oliva, A.; Quaglia, F. Poly(ether ester amide) microspheres for protein delivery: Influence of copolymer composition on technological and biological properties. *Macromol. Biosci.* **2008**, *8*, 682–689.

3. Guo, K.; Chu, C.C. Biodegradable and injectable paclitaxel-loaded poly(ester amide)s microspheres: fabrication and characterization. *J. Biomed. Mater. Res. B. Appl. Biomater.* **2009**, *89*, 491–500.
4. Shin, S.-H.; Purevdorj, O.; Castano, O.; Planell, J.A.; Kim, H.-W. A short review: Recent advances in electrospinning for bone tissue regeneration. *J. Tissue Eng.* **2012**, *3*, doi:10.1177/2041731412443530.
5. Han, D.K.; Hubbell, J.A. Synthesis of polymer network scaffolds from L-lactide and poly(ethylene glycol) and their interaction with cells. *Macromolecules* **1997**, *30*, 6077–6083.
6. Jeong, B.; Kim, S.W.; Bae, Y.H. Thermosensitive sol-gel reversible hydrogels. *Adv. Drug Deliv. Rev.* **2012**, *64*, 154–162.
7. Feng, Y.; Behl, M.; Kelch, S.; Lendlein, A. Biodegradable multiblock copolymers based on oligodepsipeptides with shape-memory properties. *Macromol. Biosci.* **2009**, *9*, 45–54.
8. Chen, X.; Zhong, H.; Jia, L.; Ling, J.; Tang, R.; Qiao, J.; Zhang, Z. Polyesteramides used for hot melt adhesives: Synthesis and effect of inherent viscosity on properties. *J. Appl. Polym. Sci.* **2001**, *81*, 2696–2701.
9. Ohya, Y.; Toyohara, M.; Sasakawa, M.; Arimura, H.; Ouchi, T. Thermosensitive biodegradable polydepsipeptide. *Macromol. Biosci.* **2005**, *5*, 273–276.
10. Roby, M.S.; Jiang, Y. Polyesteramides with Amino Acid-Derived Groups Alternating with α-Hydroxiacid-Derived Groups and Surgical Articles Made Therefrom. U.S. Patent 5,914,387, 22 June 1999.
11. Murase, S.K.; Franco, L.; del Valle, L.J.; Puiggalí J. Synthesis and characterization of poly(ester amides)s with a variable ratio of branched odd diamide units. *J. Appl. Polym. Sci.* **2014**, *131*, doi:10.1002/app.40102.
12. Vera, M.; Admetlla, M.; Rodríguez-Galán, A.; Puiggalí J. Synthesis, characterization and degradation studies on the series of sequential poly(ester amide)s derived from glycolic acid, 1,6-hexanediamine and aliphatic dicarboxylic acids. *Polym. Degrad. STable* **2005**, *89*, 21–32.
13. Ajinomoto Co., Inc.; Toray Industries, Inc. Ajinomoto and Toray to Conduct Joint Research on Biobased Nylon. Availalable online: http://www.ajinomoto.com/en/presscenter/press/detail/g2012_02_13.html (accessed on 7 January 2015).
14. Rennovia Rennovia produces RENNLON nylon, a 100% bio-based nylon-6,6 polymer. Available online: http://www.rennovia.com/LinkClick.aspx?fileticket=UKm3fT8QZ-c=&tabid=62 (accessed on 7 January 2015).
15. Cooley, J.F. Apparatus for Electrically Dispersing Fluids. U.S. Patent 692,631 A, 4 February 1902.
16. Cooley, J.F. Electrical Method of Dispersing Fluids. US Patent 745,276 A, 24 November 1903.
17. Hagiwara, K. Process for Manufacturing Artificial Silk and other Filaments by Applying Eletric Current. US Patent 1,699,615 A, 22 January 1929.
18. Formhals, A. Process ad Apparatus for Preparing Artificial Threads. US Patent 1,975,504 A, 2 October 1934.
19. Li, D.; Xia, Y. Electrospinning of nanofibers: Reinventing the wheel? *Adv. Mater.* **2004**, *16*, 1151–1170.

20. Dhakate, S.R.; Singla, B.; Uppal, M.; Mathur, R.B. Effect of processing parameters on morphology and thermal properties of electrospun polycarbonate nanofibers. *Adv. Mater. Lett.* **2010**, *1*, 200–204.
21. Llorens, E.; del Valle, L.J.; Ferrán, R.; Rodríguez-Galán, A.; Puiggalí, J. Scaffolds with tuneable hydrophilicity from electrospun microfibers of polylactide and poly(ethylene glycol) mixtures: Morphology, drug release behavior, and biocompatibility. *J. Polym. Res.* **2014**, *21*, doi:10.1007/s10965-014-0360-4.
22. Llorens, E.; Calderón, S.; del Valle, L.J.; Puiggalí, J. Polybiguanide (PHMB) loaded in PLA scaffolds displaying high hydrophobic, biocompatibility and antibacterial properties. *Mater. Sci. Eng. C* **2015**, *50*, 74–84.
23. Planellas, M.; Pérez-Madrigal, M.M.; del Valle, L.J.; Kobauri, S.; Katsarava, R.; Alemán, C.; Puiggalí, J. Microfibres of conducting polythiophene and biodegradable poly(ester urea) for scaffolds. *Polym. Chem.* **2014**, *6*, 925–937.
24. Dhanalakshmi, M.; Jog, J.P. Preparation and characterization of electrospun fibers of Nylon 11. *Express Polym. Lett.* **2008**, *2*, 540–545.
25. Celebioglu, A.; Uyar, T. Electrospun porous cellulose acetate fibers from volatile solvent mixture. *Mater. Lett.* **2011**, *65*, 2291–2294.
26. Chen, S.-H.; Chang, Y.; Lee, K.-R.; Lai, J.-Y. A three-dimensional dual-layer nano/microfibrous structure of electrospun chitosan/poly(d,l-lactide) membrane for the improvement of cytocompatibility. *J. Memb. Sci.* **2014**, *450*, 224–234.
27. Koski, A.; Yim, K.; Shivkumar, S. Effect of molecular weight on fibrous PVA produced by electrospinning. *Mater. Lett.* **2004**, *58*, 493–497.
28. Dastidar, S.G.; Ganguly, K.; Chaudhuri, K.; Chakrabarty, A.N. The anti-bacterial action of diclofenac shown by inhibition of DNA synthesis. *Int. J. Antimicrob. Agents* **2000**, *14*, 249–251.
29. Abaas, H.A.; Serry, F.M.; El-Masry, E.M. Combating pseudomonas aeruginosa biofilms by potential biofilm inhibitors. *Asian J. Res. Pharm. Sci.* **2012**, *2*, 66–72.